MSFC-235

Capabilities and Testing of the Fission Surface Power Primary Test Circuit (FSP-PTC)

Anne E. Garber

NASA/Marshall Space Flight Center
Huntsville, AL 35824
Tel: 256-544-0665, Fax: 256-544-2216, Email: Anne.E.Garber@nasa.gov

Abstract – *An actively pumped alkali metal flow circuit, designed and fabricated at the NASA Marshall Space Flight Center, is currently undergoing testing in the Early Flight Fission Test Facility (EFF-TF). Sodium potassium (NaK), which was used in the SNAP-10A fission reactor, was selected as the primary coolant. Basic circuit components include: simulated reactor core, NaK to gas heat exchanger, electromagnetic (EM) liquid metal pump, liquid metal flowmeter, load/drain reservoir, expansion reservoir, test section, and instrumentation. Operation of the circuit is based around a 37-pin partial-array core (pin and flow path dimensions are the same as those in a full core), designed to operate at 33 kWt. NaK flow rates of greater than 1 kg/sec may be achieved, depending upon the power applied to the EM pump. The heat exchanger provides for the removal of thermal energy from the circuit, simulating the presence of an energy conversion system. The presence of the test section increases the versatility of the circuit. A second liquid metal pump, an energy conversion system, and highly instrumented thermal simulators are all being considered for inclusion within the test section. This paper summarizes the capabilities and ongoing testing of the Fission Surface Power Primary Test Circuit (FSP-PTC).*

I. INTRODUCTION

To expand the multi-mission technology base related to the use of alkali metal systems for potential surface power application, the Early Flight Fission Test Facilities (EFF-TF) team has designed, fabricated and filled a pumped alkali metal (NaK) flow circuit. The circuit is comprised of a core, heat exchanger, liquid metal pump, liquid metal flowmeter, test section, lower (load/drain) reservoir, upper (expansion) reservoir, tubing, instrumentation, and spill tray.[1] The first test matrix is designed to characterize the performance of the electromagnetic liquid metal pump, which the vendor predicted would operate at near 5% efficiency. Thirteen pump performance data points have been generated thus far, which paint a clear picture of pump operations under a variety of conditions. A power balance of the system has also been generated, which verifies the proper functioning of the NaK flowmeter.

II. PRIMARY COOLANT

Liquid metals are an attractive choice for space reactor systems as a heat transfer medium due to their high thermal conductivities, high heat capacities and low vapor pressures. NaK-78 is a eutectic mixture of 22% sodium and 78% potassium by weight with a melting point of -12.6°C and a boiling point of 785°C, making it a liquid at room temperature. While freeze/thaw issues must be considered for space operations, this low melting point makes non-nuclear ground testing simpler as the liquid metal need not be heated before it can be circulated. NaK has good compatibility with stainless steel over the temperature range to be tested (650°C maximum). NaK also has a demonstrated service history for use in space reactor systems, which include SNAP-10A, TOPAZ I & II, and the RORSAT series. One notable disadvantage of NaK lies in its volatility. It reacts when exposed to oxygen, resulting in the formation of potassium oxide, potassium peroxide and potassium superoxide, which create a crust on the surface of the NaK. Hydrogen is released when NaK is exposed to water, and the heat of reaction causes it to burn.

III. CIRCUIT HARDWARE

The key components of the FSP-PTC are identified in Figures 1 and 2. The test article is mounted on a 3 m by 2 m aluminum tilt table with a 13 cm-high lip around its

edge, which is sufficient to contain all of the NaK in the system should a leak occur. The entire unit is installed in a 9-ft vacuum chamber for testing. NaK can spontaneously combust when exposed to oxygen, a phenomenon which is exacerbated by elevated temperatures; thus, testing in a vacuum adds a layer of safety beyond the physical boundary of the chamber itself. Instrumentation, power connections, and various gases (for pump cooling, pump head pressure, valve control and heat exchanger operations) interface with chamber feedthroughs. No NaK is routed outside of the chamber.
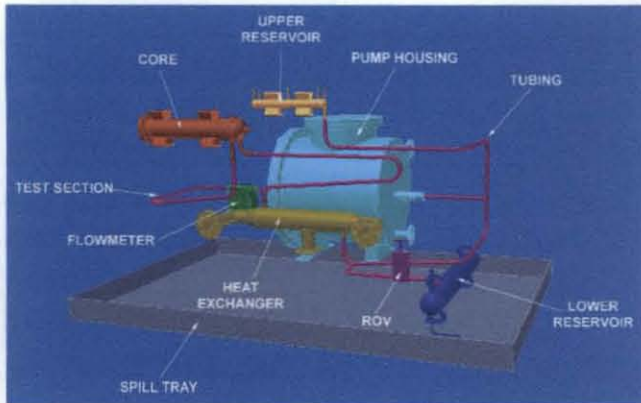

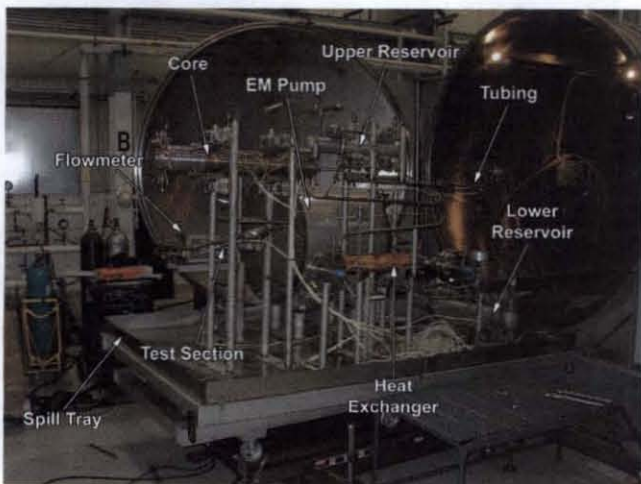Figure 1. FSP-PTC without support structure

Figure 2. FSP-PTC as constructed

All components are constructed of stainless steel. The circuit is all-welded save at a handful of locations where VCR fittings have been employed: at either side of the liquid metal flowmeter, at the expansion reservoir inlet, and just downstream of the core inlet. These fittings are also used to connect the pressure transducers and liquid level sensors to the tubing and reservoirs, respectively. Prior to the start of testing all components and tubing were proof pressure tested to greater than 300 psi and leak checked using gaseous helium to better than 10^{-9} standard

cc/sec. The potential loosening of the mechanical connections due to cyclic heating and cooling of the circuit is being monitored, and no evidence of leakage has been found to date.

III.A. Core and Thermal Simulators

The circuit was designed around the core, which is baselined from a 100-kWt Los Alamos design study[2]. In order to simplify the fabrication, integration, and testing of the hardware, the reflector drums and shields located beyond the outer pressure shell were eliminated. In addition, a partial array of the core geometry was constructed. This consists of the central three rings (37 fuel pins), resulting in a 1/3-power version of the full assembly, or 33 kW total. These reductions significantly impact the overall cost and complexity of the system (only one electromagnetic pump is needed, the requisite size of the heat exchanger and associated plumbing is reduced, and fewer thermal simulators are employed).
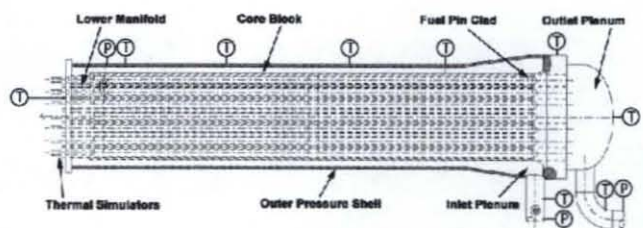

Figure 3. Core assembly

All testing performed at the EFF-TF is non-nuclear in nature, and thermal simulators are used to simulate the heat of fission[3]. The heater elements selected for this system are based on a graphite design that has been successfully used on a number of prior EFF-TF projects. Each element is 59.7 cm long and 0.775 cm in diameter. Alumina insulators are spaced every few centimeters along the length of each unit to electrically isolate the graphite from the stainless steel cladding that encompasses it. To improve thermal performance, a core face seal has been incorporated into the core assembly. The face seal permits a helium environment to be established between the graphite and the steel cladding, significantly improving the thermal coupling between them.

Fully instrumented thermal simulators (e.g. incorporating thermocouples at multiple axial locations) are undergoing development.[3] If this effort is successful, the central thermal simulator will be replaced with a fully-instrumented element for additional characterization of the test article during heated operations. Figure 4 illustrates a thermal simulator prior to installation in its steel cladding.
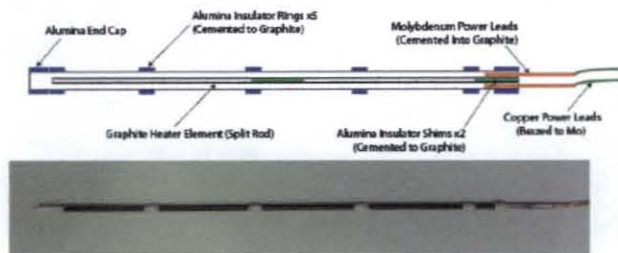
Figure 4. Thermal simulator

The thermal simulators are arranged in zones that are connected to individual power supplies (one power supply per zone). Each power supply is rated for 15 kW of DC power delivered via 150 V at 100 A maximum. The 37-pin core assembly is divided into four control zones as depicted in Figure 5. The grouping of heaters in these zones (series/parallel) is laid out such that the equivalent resistance attempts to maximize the power supply output capability. In this configuration, a maximum of 44 kW can be transferred to the heaters at 700°C. If additional power is required (to simulate transients), the number of zones could be increased to a maximum of twelve. This would result in 180 kW of available power.

Zone 1 - 7 Heater Elements
Zone 2 - 12 Heater Elements
Zone 3 - 12 Heater Elements
Zone 4 - 6 Heater Elements

Figure 5. Power zones

III.B. Heat Exchanger

Once the NaK is heated by the core assembly it passes into a heat exchanger to remove up to 40 kWt. The baseline for this heat exchanger was a "battleship" or facility-style design that provides significant robustness in this initial flow circuit. It is a 0.6 m long counter-flow design with NaK confined by the outer jacket and the secondary gaseous nitrogen coolant flow confined by 107 tubes (0.8 cm outside diameter) that pass through the NaK flow pool. The exchanger is equipped with temperature and pressure measurements to monitor boundary and fluid conditions. Nitrogen flow rates in excess of 0.4 kg/sec can be achieved, and a gas preheater raises the gas inlet temperature up to 490°C. The heated exhaust gas is vented to the atmosphere.
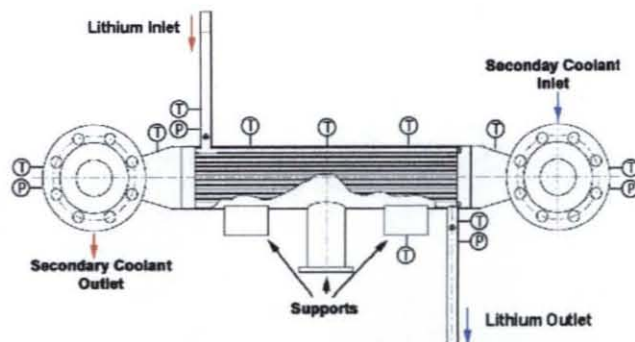

Figure 6. NaK/GN$_2$ heat exchanger

III.C. Electromagnetic Pump

NaK is circulated around the flow path by means of an electromagnetic pump, which was selected to maintain the integrity of the all-welded flow circuit with no moving parts and to build experience with a pump type that is applicable to a space power system. A general product search and open procurement in the commercial market resulted in a single pump submission that met the flow, temperature, and pressure requirements. This is a Style-VI two-stage AC conduction unit with a stainless steel 316 duct originally marketed by Mine Safety Appliance and currently offered by Creative Engineers Inc. (design dates back to the 1950's). Figure 7 shows the pump system (protective shielding removed) before integration into the pump housing. It provides continuous operation at temperatures up to 816°C, with flow control from 10% to 100% (control provided by a variable transformer).
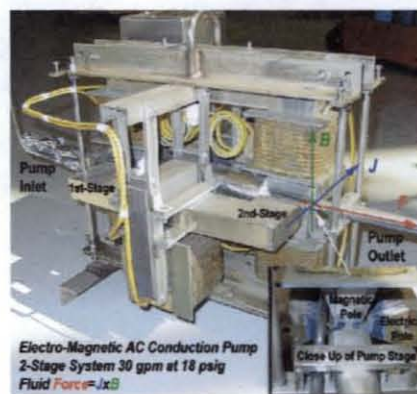

Figure 7. Electromagnetic pump

Electromagnetic pumps operate on the principle of Lorentz forces, or

$$F = JxB, \tag{1}$$

where F is force, J represents the electric field and B represents the magnetic field. In this pump, nickel bus bars have been brazed to a flattened section of the stainless

steel pump duct. NaK is a conductor of electricity, so when power is applied to the pump, current flows from one bus bar to the other through the NaK-filled duct. At the same time a magnetic flux is generated by low-temperature commercial windings on two U-shaped magnetic iron cores (perpendicular to the bus bars). The interactions of the electric and magnetic fields results in the exertion of force on the NaK and causes fluid motion. The fields have been aligned such that the maximum possible force is developed in the direction of the flow path (per the right hand rule). The commercial magnet coils are temperature-limited, and operation of the pump at the upper end of its range or at elevated NaK temperatures results in the gradual heating of the pump mechanics. The test article is operated under external vacuum pressure conditions of 10^{-3} torr or lower, eliminating natural convective cooling. The pump has been installed in a stainless steel enclosure with a gaseous nitrogen cooling purge to prevent overheating.

III.D. Reservoirs

The test article contains two reservoirs. The lower (load/drain) reservoir serves as a storage tank for NaK between tests and was used as the receptacle during the first fill of the circuit. It is separated from the flow path by means of a remotely-operated valve. During NaK transfer operations, applying argon pressure to the surface of the liquid metal forces the NaK up and into the tubes of the circuit via a dip tube, provided that the pressure in the lower reservoir is higher than the pressure in the circuit. This tube extends to 0.32 cm above the bottom of the reservoir. The applied pressure need only be very low – just two or three psi greater than circuit pressure – to achieve a controlled NaK transfer.
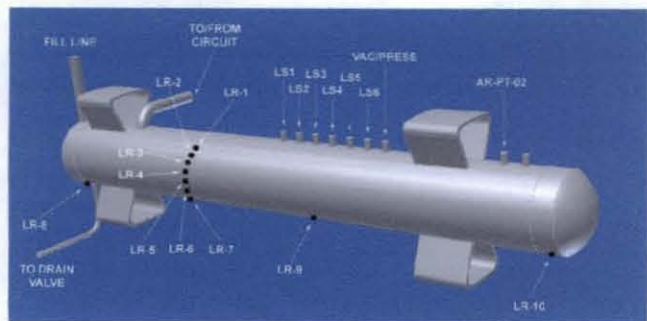

Figure 8. Lower reservoir

The function of the upper (expansion) reservoir is to contain the expansion of NaK as it is heated. At 650°C, NaK will expand to 17% above its volume at 25°C. The upper reservoir has been sized to accommodate the increase in volume of the entire circuit at 650°C with room to spare. This reservoir is also used as the argon/vacuum interface with the closed flow path. During testing, a slight argon pressure is applied here to provide the pump with head pressure (and prevent NaK from simply oscillating back and forth in the empty volume rather than circulating).

III.E. Instrumentation

Approximately 75 type-K thermocouples (TCs) are spot-welded directly to the stainless steel circuit, encompassing every component save the electromagnetic pump housing and support structure. TCs are spaced approximately eight inches apart on each section of tubing. The thermocouple wire is a high-temperature, glass-jacketed variety capable of operation up to 704°C. This instrumentation not only thoroughly monitors the temperature of all circuit components but can also serve as a rough backup for other instrumentation, such as the level sensors.

There are six pressure transducers on the NaK flow path: at the inlet and exit of the pump, core, and heat exchanger. Single transducers are located at both the expansion and fill/drain reservoir to monitor argon gas pressure, and multiple pressure sensors are employed on the nitrogen line that feeds the heat exchanger. The six sensors on the NaK flow path measure a range of 0-75 psia, and all wetted parts are stainless steel. They are temperature compensated and must remain below 162°C to operate correctly. Each of these particular transducers is set on an 18 cm standoff to prevent overheating; however, when the circuit is operating at high temperatures (above approximately 450°C), the excessive radiation from the uninsulated circuit can cause them to overheat. The circuit is scheduled to be insulated in the near future, which should drastically reduce heat loss during testing and hence prevent transducer overheating.

NaK level measurement is required in both the upper and lower reservoirs. This is accomplished using power feedthroughs that terminate in weld lips that are welded to VCR fittings. These are then mated to complementary fittings on the reservoirs. The level sensors work by completing a circuit (resistance measurement) when the level of the NaK comes into contact with the stainless steel pin of the feedthrough. As shown in Figure 9, the sensor array in the lower reservoir is designed to indicate a range of discrete volumes. The sensor heights were chosen strategically.
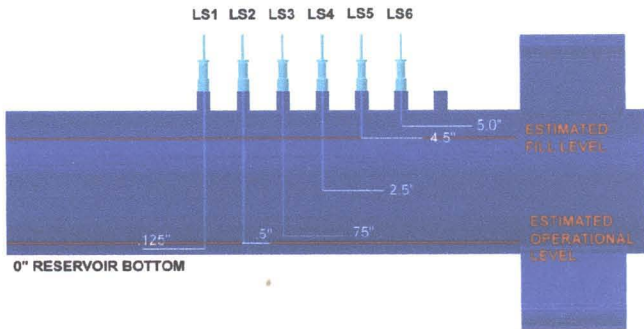
Figure 9. Level sensors in lower reservoir

IV. SIMULATION

A model of the FSP-PTC has been constructed using the Generalized Fluid System Simulation Program (GFSSP). This is a general-purpose, NASA-developed program for analyzing steady-state and transient flow rates, pressures, temperatures, and concentrations in a complex flow network. It is capable of modeling phase changes, compressibility, mixture thermodynamics and external body forces (such as gravity and centrifugal forces). The program contains subroutines for computing "real fluid" thermodynamic and thermophysical properties for twelve fluids. Other, less commonly used fluids (such as NaK) can be added by the user, so long as the required properties are known. User-written subroutines may also be incorporated within the software. As an example, the pump performance data provided by the vendor has been included in this model as a user subroutine. When a full set of experimental pump performance data has been gathered, it can be tabulated and used in place of the vendor data.

Figure 10 shows the graphical representation of the GFSSP model of the FSP-PTC. The numbered boxes are nodes, which are connected by branches. The user specifies what type of object lies between each node (tubing, orifice, etc.). The working fluid in the closed loop is NaK, and the fluid in the open loop is gaseous nitrogen. The pump, reactor core, heat exchanger, and tubing are all included in the open loop. The boundary conditions that may be set on the actual system are the same as those that may be set within the model. GN2 inlet conditions at the heat exchanger (temperature and pressure), electromagnetic pump voltage, and applied core power are all set prior to running the simulation. The boundary conditions at the exit of the heat exchanger open loop have been set to ambient.
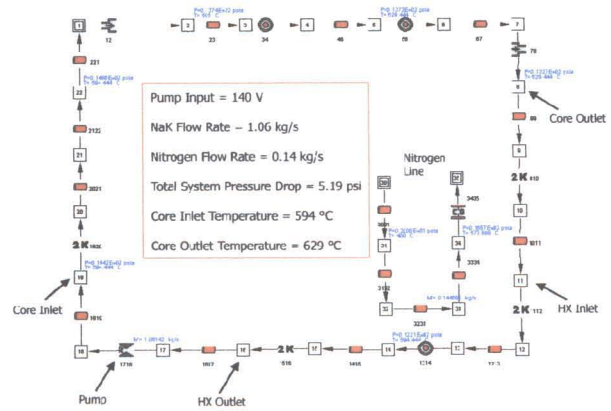

Figure 10. GFSSP model graphical representation

GFSSP employs a finite volume formation of mass, momentum, and energy conservation equations in conjunction with the thermodynamic equations of state for real fluids. Mass, energy, and species conservation equations are solved at the nodes while momentum conservation equations are solved in the branches. The system of equations describing the fluid network is solved by a hybrid numerical method that is a combination of the Newton-Raphson and successive substitution methods[4,5].

The original purpose of this model was to calculate the pressure and temperature distribution in a liquid metal cooled reactor system and thereby assist in the placement of instrumentation. The model performed this task admirably, but now that testing has begun, a few refinements are being considered. At present, heat is added to the model by directly applying it at a single node within the core. A thermal simulator could be incorporated into the overall model. More important than this, however, is the need to better match the simulation with the actual thermal environment in the chamber. As Section V.B explains, a good deal of the power applied to the core is lost to the chamber walls through radiation (the circuit is uninsulated). GFSSP is overpredicting the NaK flow rate at a given ΔP by nearly twice the experimental value, which is almost certainly due to the lack of real heat losses in the model. Simulation results can be better compared to actual test data when 1) radiation losses are included in the model, or 2) the circuit is insulated. As was previously established, preparations to insulate the test article are underway.

V. TESTING

A series of experiments are being conducted on the FSP-PTC, beginning with the execution of a pump performance test matrix. The results will be compared with performance data provided by the vendor. Following

the completion of this stage, a series of integrated system performance tests will be performed, which (in conjunction with the pump performance data) can be used to validate the GFFSP model. Finally a series of transient cases will be examined, at which point the team will be ready to incorporate new hardware components into the system via the test section. Before the test section can be removed, the interior must be cleaned of NaK. To this end, the team has procured an alkali metal cleaning system from Creative Engineers, Inc., which mixes dry steam with the NaK-wetted interior of the circuit to form hydroxides. The machinery may also be used to react the bulk of the NaK, which would be done within the load/drain reservoir. Once the circuit has been cleaned the test section may be removed at its mechanical connection points. The hardware components being considered for use includes a Stirling engine heat exchanger or an induction-style liquid metal pump. A second, smaller test article designed to characterize the flow of NaK around a single resistance heater may also be added to the test section.

V.A. Pump Performance

The pump performance test matrix is intended to characterize the developed NaK pressure and flow rate as a function of pump power over a range of NaK temperatures. The aforementioned variable transformer allows the test engineer to specify precisely how much voltage is applied to the pump, with 235 V being the maximum. Table 1 shows the data points to be tested; boxes in yellow indicate data that have already been obtained. The matrix is designed to be run one row (NaK temperature) at a time. The numbers in each box indicate which pump setting is to be run first, second, etc. at the given temperature. This introduces a degree of randomness into the proceedings and helps to prevent unintentional trending due to a linear progression of data points. In Table 1, "NaK Flow Temp" is the temperature of the NaK within the liquid metal pump. Because the circuit is not insulated and the heat exchanger lies between the core and the pump, there is some difference between the NaK temperatures at these locations.

TABLE 1

Pump Performance Test Matrix

		EM Pump Voltage			
		100V	140V	200V	235 V
	350°C	4	2	3	1
	375°C	3	1	4	2
	400°C	1	3	2	4
NaK	425°C	2	4	1	3
Flow	450°C	4	2	3	1
Temp	475°C	3	1	4	2
	500°C	1	3	2	4
	525°C	2	4	1	3
	538°C	4	2	3	1

In a typical pump performance test, the desired NaK temperature is selected first. This can be any of the temperatures listed along the vertical in Table 1. GFSSP is used to generate a set of ballpark system settings needed to bring the NaK up to this temperature (applied core power, GN_2 temperature at the inlet of the heat exchanger, and GN_2 flow rate). It is undesirable to rapidly apply a great deal of power to a cold core, and gaseous nitrogen cannot be heated instantaneously, so these settings are increased over a span of time until the final values are reached. (For example, power is applied to the core at a maximum rate of 1 kW/min). The pump voltage is set to whichever value the test matrix dictates should be first for the given NaK temperature. Core power and heat exchanger GN_2 settings are adjusted until the NaK temperature appears to be settling at approximately the correct temperature. The NaK temperature is allowed to come to steady state, at which point the pump voltage is changed to the second proscribed value. This procedure is followed until all data points in the row have been obtained (or until the test must be shut down, usually due to time constraints). The system is declared to have reached steady state when the NaK temperature at a given location has changed by no more than 4°C over a span of one hour. To determine the veracity of this definition, a simple test was run in which the test article was allowed to run at a single set of conditions for more than six hours. Figure 11 shows the NaK temperature at various locations around the circuit, the NaK flow rate, and pump voltage during this test. The sudden change in the NaK flow rate (represented by the blue line) corresponds to an unanticipated 'blip' in the power that was supplied to the EM pump.
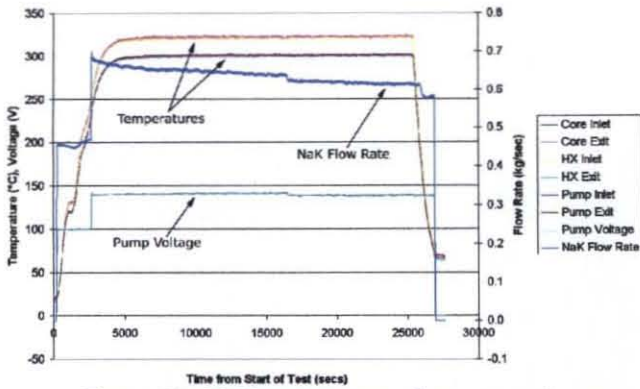
Figure 11. NaK temperature, flow rate and pump
voltage during steady state test

Figure 12. Pump performance data

As Figure 11 indicates, NaK temperatures stabilize fairly quickly once final core power and pump voltage levels have been reached. Data from all tests have shown that surface temperatures around the circuit level off together, so when the temperature at one location has come to steady state, all NaK temperatures can be assumed to be at steady state as well. In the all-day steady state test, the NaK flow rate did not stabilize as quickly as the temperatures did. NaK pressures, not shown on this graph, also took longer than the temperatures to stabilize although not nearly as long as the flow rate. Due to time constraints on the project, it is not possible for the test engineers to wait until the all these values have come to steady state before taking a data point. Doing so would limit the team to collecting only one data point per day. For the purposes of these tests, it has been determined that the pressures and temperatures are sufficiently stable to warrant declaring "steady state" when the aforementioned conditions have been met.

Data is averaged over the length of the steady state windows to produce the data points used in the pump performance graphs below (Figures 12 and 13). For three of these thirteen data points, steady state data was not available for a full hour. In those cases the average was taken over the span of time for which the temperature at the core exit did not vary more than 4°C (the time span was at least 2500 seconds for all three points). No averages were taken when greater temperature transients were observed.
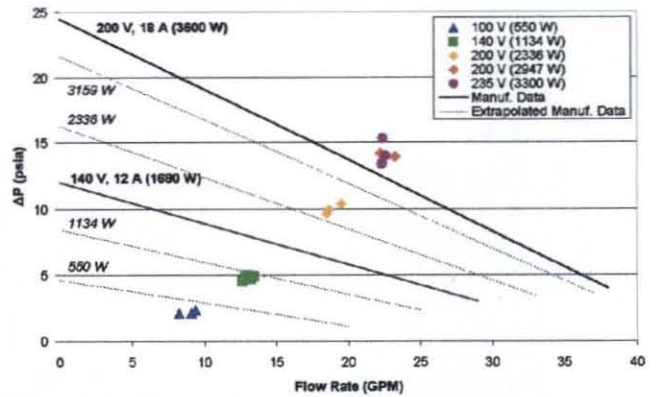
Pump performance data is plotted in Figure 12, with NaK flow rate as measured by the liquid metal flowmeter on the x-axis and the pressure developed by the liquid metal pump on the y-axis. Data provided by the pump vendor, which was taken experimentally in the 1970s, is represented by the continuous lines. Since this is an AC electromagnetic pump, the applied power represented by these lines must be assessed carefully. However, due to the location where the current and voltage were measured in the 1970s tests, the VI approximation can be made for the purposes of comparison with FSP-PTC test data. In Figure 12, FSP-PTC data points have been grouped by applied pump voltage, with the average applied pump power for each group also indicated. Pump performance data for each of these power levels was extrapolated from the vendor's curves and are represented by the dashed lines. (Note that 3159 W is the average pump power of *all* the data points in the upper right group.)

The NaK flow rate and developed pressure increase in a roughly parabolic fashion as applied pump power is increased. (The two 200 V data points that are not located near their main group will be discussed later in this section.) As was previously stated, the real pump power for each of the vendor curves is only approximated from the given current and voltage; therefore, the test engineers have been matching the *voltages* from each of these curves. To illustrate: the applied current for the group of 140 V data points (green squares) was approximately 7.8 amps as opposed to the 12 amps shown on the manufacturer's curve. This group had an average pump power of 1134 W and logically falls below the 140 V, 12 A (~1680 W) line. When the extrapolated 1134 W line is added to the graph, the data points taken at this power level fall very close to it. The same is true for the 100 V group and most of the 200 V group. It should also be noted that the vendor data were generated at a NaK temperature of 566°C. The maximum temperature that can currently be attained in the FSP-PTC is 527°C. This

may result in some differences between the FSP-PTC data and the vendor curves. One would expect that the data would not fall directly on the curves due to the approximations and differences described here.
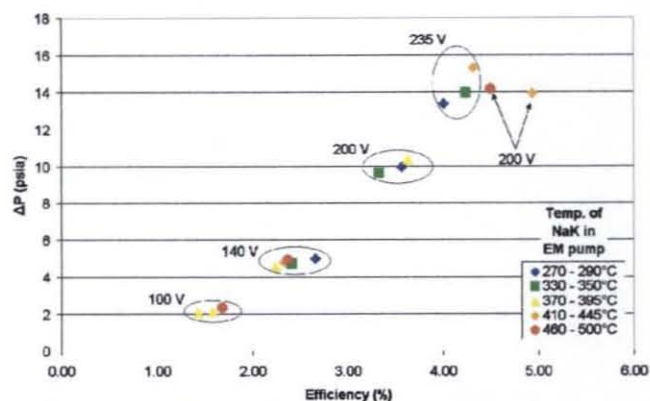

Figure 13. Pump efficiency

Figure 13 is a plot of developed NaK pressure versus pump efficiency. To illustrate the effect of NaK temperature on pump performance, the data points have been grouped by temperature rather than applied voltage/power. Pump efficiency is calculated per the following equation:

$$Eff(\%) = \frac{VolumetricFlowRate\left(\frac{m^3}{s}\right) \times \Delta P(Pa)}{PumpPower(W)} \quad (2)$$

where ΔP is the NaK pressure rise and pump power is the wattage that is applied for pump operations. The data in Figure 13 clearly shows that the pump performs more efficiently when operating near its maximum rating. In Figure 12, attention was drawn to two 200 V data points (red diamonds) that fell outside of their main grouping. At these particular points the temperatures of the NaK in the pump were 428°C and 493°C, respectively – hotter than the rest of the points taken at this voltage. No temperature data is taken on the pump mechanics themselves (most temperature measurements within the pump housing have proven to be either noisy or unreliable), but test data shows that the pump was drawing a higher current at these two points than at the other three, resulting in a higher overall applied pump power.

The vendor has stated that the electromagnetic pump will operate more efficiently at NaK temperatures greater than 427°C. (At 358°C and below, nickel has a ferromagnetic quality[6] which can negate some of the flux generated by the pump's electromagnetic windings.) The two outstanding 200 V points were taken above this NaK temperature threshold, while the other three were below it.

It is difficult to determine just how much of the separation is due to temperature-improved efficiency as opposed to the increase in overall power draw (and also since the most efficient 200 V data point was not the warmest of the five 200 V points). Additionally, it is not known precisely how long it takes for the pump to "warm up"; the nitrogen gas that flows through the pump housing is cold, and will vie with the heated NaK to affect the overall pump temperature. Still, Figure 13 does appear to indicate a general trend toward higher efficiencies as temperature increases in each group of points. In the case of the data points taken at 235 V, developed pressure rises with increasing NaK temperature, but pump efficiency does not increase a great deal. This seems to suggest that the pump is already operating at near-best efficiency when the maximum possible power is applied, leaving less room for an increase in performance as NaK temperature rises. However, only three data points have been taken at this voltage setting, and more data will help paint a clearer picture of pump behavior at 235 V.

V.B. Power Balance

The execution of the pump performance matrix provides an excellent opportunity to evaluate the liquid metal flowmeter, which is difficult to calibrate. The only way to do this is to pass a known volume of NaK through it over a set amount of time. This has not been done for this particular piece of equipment; however, the vendor has provided a correlation based on previous flowmeter experience. A power balance across the heat exchanger can be used to get an idea of whether or not the values being reported by the flowmeter are in the right ballpark. NaK flow rate can be determined through use of the heat exchanger and the following relationship:

$$Q = \dot{m}C_p\Delta T . \quad (3)$$

In a well insulated heat exchanger the energy coming in would be equal to that removed. Since the FSP-PTC is not insulated, the energy input to the system is equal to the energy removed by the heat exchanger plus thermal losses:

$$Q_{NaK} = Q_{Nitrogen} + Q_{Losses} . \quad (4)$$

Q_{losses} is comprised of energy losses due to conduction and radiation, but conduction has been omitted from the following assessment for several reasons. First, the flow circuit is supported by a steel structure, but the connection points are few and cover a small surface area. Second, there are no thermocouples on the support structure to measure the ΔT needed for conduction calculations. Finally, as temperature increases, the losses due to

radiation far outweigh conductive losses due to the 4th power temperature factor in Eq. (5):

$$Q_{rad} = \varepsilon \sigma A \left(T_s{}^4 - T_{sur}{}^4 \right). \tag{5}$$

ε is the emissivity of stainless steel, σ is Bolzmann's constant (5.67×10^{-8} W/m-K), A is the radiative surface area, T_s is the surface temperature of the test article and T_{sur} is the temperature of the vacuum chamber wall.
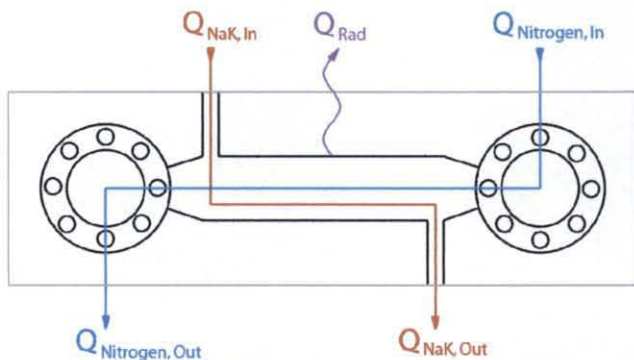

Figure 14. Heat exchanger power balance

Let us consider the heat exchanger as a control volume (Figure 14). All energy that enters the volume must also leave the volume (if there is no energy storage). As Eq. (4) states, energy enters the heat exchanger via heated NaK and is dissipated through the nitrogen flow and radiation. The inlet and outlet temperature of the gas and the gas flow rate are measured, and the specific heat is known for the gas. For simplicity, the surface temperature of the heat exchanger is taken as the average of the NaK inlet and exit temperatures. NaK mass flow rate is constant throughout the circuit. Therefore, if $Q_{losses} = Q_{rad}$, the NaK mass flow rate can be determined from Eq. (6):

$$\dot{m}_{NaK} = \frac{\dot{m}_{GN2} C_{p,GN2} \Delta T_{GN2} + \varepsilon \sigma A \left(T_s{}^4 - T_{sur}{}^4 \right)}{C_{p,NaK} \Delta T_{NaK}} \tag{6}$$
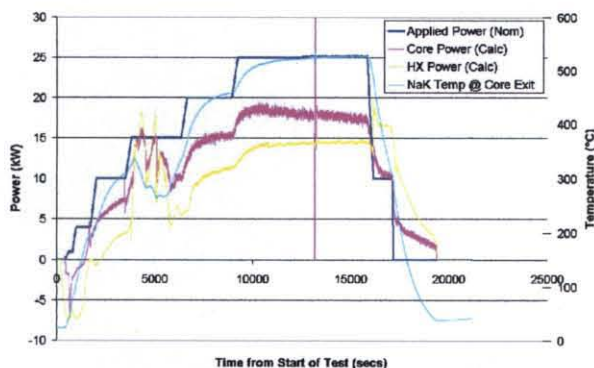

Figure 15. Power and temperature, 527°C test

Figure 15 shows power and temperature data from one pump performance test. The maximum power applied to the core was 25 kW, which brought the NaK temperature at the exit of the core (the hottest location in the circuit save within the core itself) up to 527°C. It is immediately obvious that there is a significant thermal loss in the system, represented by the gap between the power applied to the core (dark blue) and the power removed by the heat exchanger (yellow). At 15000 seconds, when the NaK temperature had reached steady state, the difference between the two is almost 11 kW, and the flowmeter was reporting a NaK flow rate of 13.36 GPM (0.64 kg/sec). Using an emissivity of 0.4[7] (oxidized stainless steel at 800 K), an estimated chamber wall temperature of 25°C and a heat exchanger surface area of 0.2917 m[2], Eq. (5) yields the energy lost by radiation at the heat exchanger as 2581 W. Using the experimental data for nitrogen temperatures at the inlet and outlet, calculated specific heats[8], and the measured nitrogen flow rate, the energy removed by the heat exchanger is found to be 15108 W. When these two losses, NaK temperatures and their respective specific heats[8] are incorporated into Eq. (6), the calculated NaK flow rate is 13.89 GPM (0.66 kg/sec). Considering that conductive heat losses have been omitted, the emissivity of stainless steel (at this temperature) ranges from 0.24 to 0.67[7], and other approximations, it appears that the flowmeter is indeed reporting reasonable values. Insulating the circuit will improve this assessment by reducing the uncertainty contribution associated with the radiation losses. Steps are also being taken to acquire temperature data on the test article support structure, which will allow for the quantification of heat loss by conduction.

VI. CONCLUSIONS

Testing has begun on the Fission Surface Power Primary Test Circuit. A maximum NaK temperature of 527°C has been reached with flow rates in excess of 1.1 kg/sec reported. The first set of data points from the pump performance test matrix indicate that the liquid metal pump operates in the approximately 1.5 - 5% efficiency range. Efficiency improves as greater power is applied to the pump and also with increasing NaK temperature, although the latter effect is not evident at low pump voltages. Thus far, results indicate that the increase in efficiency does occur near the vendor-reported temperature of 427°C. This matrix is not yet complete, and it is hoped that more tests will establish a better understanding of pump performance at the highest possible applied power levels. A basic power balance indicates that the liquid metal flowmeter, which has not been calibrated, is reporting reasonable values. It is expected that the flow

rates reported by the meter will better match the calculated values once the circuit has been insulated. Insulating the circuit will also prevent pressure transducer overheating and will enable the test engineers to begin comparing test data against the results of the GFSSP simulation. Upon completion of the pump performance matrix, integrated system and transient cases will be performed, followed by the eventual inclusion of new hardware components in the test section.

ACKNOWLEDGMENTS

The author would like to acknowledge the contributions of Thomas Godfroy, Roger Harper, Dr. Alok Majumdar, Stan McDonald, Gene Fant, Jason Berry, Dr. Kenneth Webster, James Martin, Melissa Van Dyke, and Dr. Shannon Bragg-Sitton for their many hours of effort on this project.

NOMENCLATURE

A	Amps
AC	Alternating current
B	Magnetic field
°C	Degrees Celsius
C_P	Specific heat
cc	Cubic centimeters
cm	Centimeters
DC	Direct current
F	Force
GN_2	Gaseous nitrogen
GPM	Gallons per minute
J	Electric field
K	Kelvin
kg	Kilograms
kW	Kilowatts
kWt	Kilowatts thermal
m	Meters
$\dot{m}$	Mass flow rate
NaK	Sodium-potassium
P	Pressure
psi	Pounds per square inch
psia	Pounds per square inch, absolute
Q	Energy
s	Seconds
sec	Seconds
T	Temperature
TC	Thermocouple
V	Volts
W	Watts

REFERENCES

1. Anne E. Garber and Thomas J. Godfroy, "Design, Fabrication and Integration of a NaK-Cooled Circuit", Paper 6331, *Proceedings of ICAPP 2006*, Reno, NV.

2. David I. Poston, "A 100-kWt NaK-Cooled Space Reactor Concept for an Early-Flight Mission", *Space Technology and Applications International Forum – STAIF 2003*, American Institute of Physics (2003).

3. S.M. Bragg-Sitton, J. Farmer, D. Dixon, et al, "Development of High Fidelity, Fuel-Like Thermal Simulators for Non-Nuclear Testing", *Space Technology and Applications International Forum – STAIF 2007*, American Institute of Physics (2007).

4. Majumdar, A. K., "A Generalized Fluid System Simulation Program to Model Flow Distribution in Fluid Networks", Paper no. AIAA 98-3682, 34th AIAA/ASME/SAE/ASEE Joint Propulsion Conference and Exhibit (1999).

5. Majumdar, A.K., "A Second Law Based Unstructured Finite Volume Procedure for Generalized Flow Simulation", Paper no. AIAA 99-0934, 37th AIAA Aerospace Sciences Meeting Conference and Exhibit (1999).

6. Davis, J.R., *ASM Specialty Handbook: Nickel, Cobalt and Their Alloys*, ASM International, Materials Park, OH (2000).

7. F. P. Incropera, D. P. DeWitt, *Fundamentals of Heat and Mass Transfer, Third Edition*, Chapter 12, John Wiley & Sons, New York (1990).

8. Cengel, Y.A., Boles, M.A., *Thermodynamics: An Engineering Approach*, p. 764-765, McGraw-Hill, New York (1989).

9. Burdi, G. F., *SNAP Technology Handbook Volume 1, Liquid Metals*, Atomic International Report *No. NAA-SR-8617* (August, 1964).